Adenosine signaling and its downstream target mod(mdg4) modify the pathogenic effects of polyglutamine in a *Drosophila* model of Huntington's disease

Yu-Hsien Lin[1,2*], Houda Ouns Maaroufi[1,2], Lucie Kucerova[1], Lenka Rouhova[1,2], Tomas Filip[1,2], Michal Zurovec[1,2*]

[1]Biology Centre of the Czech Academy of Sciences, Institute of Entomology, Ceske Budejovice, Czech Republic, [2]Faculty of Science, University of South Bohemia, Ceske Budejovice, Czech Republic

*Correspondence and requests for materials should be addressed to Y.H.L. (email: r99632012@gmail.com) and M.Z. (email: zurovec@entu.cas.cz).

Abstract

Dysregulation of adenosine (Ado) homeostasis has been observed in both rodent models and human patients of Huntington's disease (HD). However, the underlying mechanisms of Ado signaling in HD pathogenesis are still unclear. In the present study, we used a *Drosophila* HD model to examine the concentration of extracellular Ado (e-Ado) as well as the transcription of genes involved in Ado homeostasis and found similar alterations. Through candidate RNAi screening, we demonstrated that silencing the expression of adenosine receptor (*adoR*) and equilibrative nucleoside transporter 2 (*ent2*) not only significantly increases the survival of HD flies but also suppresses both retinal pigment cell degeneration and the formation of mutant Huntingtin (mHTT) aggregates in the brain. We compared the transcription profiles of *adoR* and *ent2* mutants by microarray analysis and identified a downstream target of AdoR signaling, *mod(mdg4)*, which mediates the effects of AdoR on HD pathology in *Drosophila*. Our findings have important implications for the crosstalk between Ado signaling and the pathogenic effects of HD, as well as other human diseases associated with polyglutamine aggregation.

Introduction

Adenosine (Ado) is one of the most common neuromodulators in the nervous system of vertebrates as well as invertebrates and modulates synaptic transmission(Cunha, 2001; Dunwiddie & Masino, 2001). Under normal conditions, the extracellular Ado (e-Ado) concentration is in the nanomolar range, which is sufficient to modulate the appropriate adenosine receptors (AdoRs) in the brain cells tonically(Fredholm, 2007). However, under pathological circumstances the e-Ado level may increase up to 100-fold. In these conditions, Ado functions as an imperfect neuroprotector; in some cases it may be beneficial and in others may worsen tissue damage(Picano & Abbracchio, 2000). Recent experiments with knockout mice for all four *adoRs* demonstrated that Ado signaling is less involved in baseline physiology and likely more crucial for its roles as a signal of stress, damage, and/or danger(Xiao, Liu, Jacobson, Gavrilova, & Reitman, 2019). It has also been suggested that Ado signaling is mainly engaged when an allostatic response is needed(Cunha, 2019).

Due to its impact on important physiological functions in the brain, e-Ado signaling has attracted attention as a possible therapeutic agent in Huntington's disease (HD)(Lee & Chern, 2014), a dominant hereditary neurodegenerative disorder caused by a mutation in the Huntingtin gene (*htt*). Mutated HTT protein (mHTT) contains an expanded polyglutamine (polyQ) tract encoded by 40 to more than 150 repeats of CAG trinucleotide(Vonsattel & DiFiglia, 1998). Although mHTT is ubiquitously expressed in the central nervous system (CNS) and peripheral cells in HD patients, it predominantly affects striatal neurons that contain a higher density of adenosine receptors A2A ($A_{2A}R$) and A1 (A_1R)(D. Blum, R. Hourez, M.-C. Galas, P. Popoli, & S. N. Schiffmann, 2003). Several studies have demonstrated that the abnormality of AdoRs activity, especially $A_{2A}R$ in the striatum, contributes to HD pathogenesis(David Blum et al., 2018; Gomes, Kaster, Tome, Agostinho, & Cunha, 2011). In addition, the alteration of adenosine tone and the upregulation of striatal equilibrative nucleoside transporters (ENTs), facilitating Ado transport across the cytoplasmic membrane, suggest that e-Ado concentration could serve as a HD biomarker for assessing the initial stages of neurodegeneration(Guitart et al., 2016; Kao et al., 2017a). However, the complexity of the system modulating Ado metabolism

and the crosstalk between individual AdoRs, as well as their interactions with purinergic (P2) or dopamine receptors, impedes the characterization of HD pathophysiology and downstream mechanisms of e-Ado signaling (Anderson & Nedergaard, 2006; Tyebji et al., 2015).

Drosophila expressing human mHTT has previously been demonstrated as a suitable model system for studying gene interactions in polyQ pathology, and has been used to elicit a number of modifiers for symptoms of HD (Lewis & Smith, 2016; Steffan et al., 2001). *Drosophila* e-Ado signaling is a relatively simple system compared to mammals; it contains a single AdoR isoform (cAMP simulation) and lacks P2X receptors (Fountain, 2013; Kucerova et al., 2012). Human homologs of the *Drosophila* genes involved in the regulation of Ado homeostasis and AdoR are shown in Fig. S1. The lack of adenosine deaminase 1 (ADA1) in *Drosophila* indicates that adenosine deaminase-related growth factors (ADGFs, related to ADA2), together with adenosine kinase (AdenoK), are the major metabolic enzymes converting extra- and intra-cellular adenosine to inosine and AMP, respectively (Maier, Galellis, & McDermid, 2005; Stenesen et al., 2013; Zurovec, Dolezal, Gazi, Pavlova, & Bryant, 2002). e-Ado signaling in *Drosophila* is involved in regulating various physiological and pathological processes, including modulation of synaptic plasticity, JNK-mediated stress response, hematopoiesis, and metabolic switching upon immune challenges (Bajgar et al., 2015; Knight et al., 2010; Poernbacher & Vincent, 2018).

In the present study, we performed a candidate RNAi screen examining the role of Ado signaling in a *Drosophila* HD model. We co-expressed exon 1 with a polyglutamine tract of normal human *htt* Q20 or pathogenic *mhtt* Q93(Steffan et al., 2001) together with *UAS-RNAi* or *UAS*-overexpression constructs specific for *adoR*, Ado transporters, and Ado metabolic enzymes in *Drosophila*. We demonstrated that the downregulation of *adoR* and *ent2* expression reduces cell death, mortality and the formation of mHTT aggregates. In addition, we identified a number of differentially-expressed genes in response to Ado signaling and showed that *mod(mdg4)* is a downstream target of AdoR that mediates its effect in HD pathogenesis.

Results

Phenotypes of *Drosophila* expressing mHTT

To verify the effect of mHTT expression on *D. melanogaster*, we used a *UAS/GAL4* system for targeted gene expression. Flies overexpressing normal exon 1 from human huntingtin (Q20 HTT), or its mutant pathogenic form (Q93 mHTT), were driven by the pan-neuronal driver, *elav-GAL4*. The results showed that expression of mHTT under the *elav-GAL4* driver in the *Drosophila* brain is not lethal during the larval stage (Fig. S2A) but reduces both the adult eclosion rate (Fig. S2B) and adult lifespan (Fig. S2C). These results are consistent with previous observations(Song et al., 2013).

Disturbance of extracellular adenosine (e-Ado) homeostasis in HD larvae

A recent study of human HD patients reported a reduced concentration of e-Ado in the cerebrospinal fluid (Kao et al., 2017b). To determine whether e-Ado levels are also altered in HD *Drosophila*, we compared e-Ado levels in the hemolymph of last-instar larvae ubiquitously expressing Q20 HTT and Q93 mHTT driven by the *daughterless-Gal4* driver (*da-GAL4*). The results showed that the e-Ado concentration in the hemolymph of Q93-expressing larvae was significantly lower compared to larvae expressing Q20 or control *da-GAL4* (Fig. 1A).

Since e-Ado concentration may be associated with the level of extracellular ATP (e-ATP), we also examined its titer in the hemolymph of larvae with the same genotypes as the above experiment. As shown in Fig. 1B, there was no significant difference in e-ATP levels between Q20, Q93, and control *da-GAL4* larvae. We thus postulated that the lower level of e-Ado in Q93 larvae might be affected by changes in proteins involved in Ado metabolism or transportation.

Altered transcriptions of genes involved in Ado homeostasis in HD *Drosophila*

Earlier reports have shown that the expression of several genes involved in Ado homeostasis, including Ado receptor, transporters, and genes involved in Ado metabolism, are abnormal in human HD patients as well as in HD mice (Glass, Dragunow, & Faull, 2000; Martinez-Mir, Probst, & Palacios, 1991; Mievis, Blum, & Ledent, 2011). Since

homologous proteins have also been shown to control Ado homeostasis in flies (Fig. S1), we compared the expression of three *Drosophila adgf* genes (*adgf-a*, *adgf-c*, *adgf-d*), adenosine kinase (*adenoK*), adenosine transporters (*ent1*, *ent2*, *ent3*, *cnt2*), and adenosine receptor (*adoR*) in the brains of Q93- and Q20-expressing larvae. The results showed that the expression of *adgf-a* and *adgf-d*, as well as transporters *ent1*, *ent2*, and *ent3* in the brain of Q93 larvae were significantly lower than in Q20 larvae (Fig. 1D). The expression of *cnt2* and *adoR* showed no difference between Q93 and Q20 larvae.

In order to assess progressive changes in transcription profiles associated with HD pathogenesis, we further examined the expression of genes involved in Ado homeostasis in the heads of 5- and 15-day-old adults, roughly corresponding to early- and late-stage HD (Fig. S2C). Unlike in the larval stage, the expression of metabolic genes *adgf-c*, *adgf-d*, and *adenoK*, and transporter *ent1*, in five-day-old adults was found to be higher in Q93 flies than Q20 flies (Fig. 1E). In addition, 15-day-old Q93 flies showed higher expression of *adgf-d* and *adenoK* (Fig. 1F). Previous studies in *Drosophila* have shown that the downregulation of the transporter *ents* decreases e-Ado concentration (Bajgar et al., 2015; Poernbacher & Vincent, 2018); hence, the reduced expression of three *ent* genes could explain why the e-Ado level is lower in Q93 larvae. Moreover, it has also been shown that the expression of *adgfs* as well as *adenoK* follows the levels of e-Ado upon stress conditions (Bajgar & Dolezal, 2018; Zuberova, Fenckova, Simek, Janeckova, & Dolezal, 2010), suggesting that the lower expression of *adgfs* in Q93 larvae and the higher expression in Q93 adults might be a consequence of elevated e-Ado concentrations resulting from HD pathogenesis.

Functional characterization of Ado homeostasis and signaling in HD flies

To understand the effects of alterations in Ado homeostasis on polyQ pathology, we used the pan-neuronal driver, *elav-GAL4*, for RNAi-mediated silencing of the genes involved in Ado transport, metabolism, and *adoR* in Q93-expressing flies and assessed their survival and formation of mHTT aggregates. In addition, we also co-expressed Q93 with RNAi transgenes in the eyes by using the *gmr-GAL4*(Kuo, Ren, Lao, Edgar, & Wang, 2013; Mugat, Parmentier, Bonneaud, Chan, & Maschat, 2008) driver and compared levels of retinal pigment cell degeneration.

Silencing the transcriptions of Ado metabolic enzymes showed that only the RNAi of *adgf-D* increased the number of eclosion rate (Fig. 2A). Silencing *adgf-A* and *adenoK*, but not *adgf-D* or *adgf-C* RNAi, extended the adult lifespan of Q93-expressing flies (Fig. 2B). To ensure that the mortality of the HD flies was mainly caused by Q93 expression and not by RNAi constructs, we recorded the survival of flies co-expressing normal *htt* Q20 together with RNAi transgenes until all corresponding experimental flies (expressing Q93 together with RNAi constructs) died (Fig. S3A). However, silencing *adgfs* or *adenoK* only affected survival and did not significantly influence mHTT aggregation (Fig. 2C&D) or retinal pigment cell degeneration (Fig. 2E).

Next, we examined the RNAi silencing of *adoR* and Ado transporters in Q93 and control Q20 flies. The results showed that knocking down the expression of *adoR* as well as two transporters, *ent1* and *ent2*, significantly increased the eclosion rate (Fig. 3A) and adult lifespan (Fig. 3B). The RNAi silencing of *ent2* and *adoR* extended the lifespan of HD flies to 30 and 40 days, respectively, which is about 1.5~2 times longer than that of HD flies. In contrast, knocking down *cnt2* expression did not change the viability of HD flies, and knocking down *ent3* did not influence the eclosion rate, although it increased mortality and shortened the lifespan of adult HD flies. The survival of control flies expressing Q20 with individual RNAi constructs are shown in Fig. S3B. mHTT aggregation was significantly reduced (to 50%) in *adoR* RNAi flies (Fig. 3C&D), and a similar suppression of mHTT aggregate formation was also observed in 20-day-old HD flies (Fig. S4). An examination of eye phenotypes in *ent2* RNAi flies showed a significant reduction in retinal pigment cell death (Fig. 3E), but surprisingly we did not observe a significant rescue of cell death by silencing *adoR* (Fig S5). We therefore postulated that it might be due to insufficient RNAi efficiency for suppressing AdoR signaling in the eye. To test this, we combined Q93 flies with the *adoR* RNAi transgene under a *adoR* heterozygote mutant background ($AdoR^1$/+) or with $AdoR^1$ homozygote mutant, and both showed significantly decreased retinal pigment cell degeneration similar to *ent2*–RNAi flies (Fig. 3E).

To further validate the RNAi results, we studied flies simultaneously expressing Q93 and overexpressing *ent2*, *adoR*, *adgf-A*, and *adenoK* in the brain and assessed the adult lifespans. Since silencing these genes extended the lifespan of HD flies (Figs. 2B&3B), we

expected the opposite effect upon overexpression. As shown in Fig. S6A, *ent2* overexpression significantly increased the mortality of early-stage HD flies; the survival of 5-day-old flies dropped to 60% for HD flies in contrast to 90% for Q93 control flies, and the lifespan of HD flies was significantly shorter than control flies expressing either Q93 alone or together with *gfp* RNAi. Consistently, we co-expressed strong and weak *adoR* overexpressing transgenes with Q93 and both significantly increased the mortality and shortened the lifespan of Q93 flies. The effects of shortening the lifespan were more severe than with *ent2* overexpression. Nevertheless, the increase in mortality by *adgf-A* and *adenoK* overexpression was not as strong as that caused by *ent2* and *adoR* overexpression, although both still showed a significant difference to either Q93 control or Q93/*gfp* RNAi control by weighted log-rank test (Fig. S6B). Hence, we concluded that overexpressing the examined genes enhances the effect of mHTT, resulting in the increased mortality of HD flies. Our results demonstrate that the overexpression and silencing of *ent2* or *adoR* has a stronger influence over HD pathology than genes involved in Ado metabolism.

Interactions of AdoR with ENT1 and ENT2

In order to investigate whether there is a synergy between the effects of AdoR and ENTs, we co-expressed *adoR* RNAi constructs with *ent1* RNAi or *ent2* RNAi in Q93-expressing flies. As shown in Fig. 4A, the silencing of both *ent2* and *adoR* has the same effect as silencing only *adoR*, indicating that ENT2 and AdoR are in the same pathway. Interestingly, the double knockdown of *ent1* and *adoR* shows a sum of individual effects on lifespan which is longer than the knockdown of *adoR* alone. There seems to be a synergy between ENT1 and AdoR suggesting that ENT1 may have its own effect, which is partially independent from AdoR signaling.

Next, we investigated our hypothesis that the source of e-Ado, which contributes to AdoR activation in Q93 flies, is mainly intracellular and released out of the cells by ENTs. We conducted an epistasis analysis by combining mHTT with *adoR* overexpression and *ent1* or *ent2* RNAi. The results showed that *adoR* overexpression increased the mortality of Q93 flies while the combination of *adoR* overexpression with either *ent1* or *ent2* RNAi minimized the increased mortality caused by *adoR* overexpression (Fig. 4B). Notably, Q93 flies expressing *ent2* RNAi and overexpressing *adoR* had the longest lifespan

in comparison to Q93 control or *ent1* RNAi flies. These results suggest that AdoR signaling needs functional Ado transportation to carry out its effect and thus the Ado efflux from these cells is needed for AdoR activity (Fig. 4C&D). The source of e-Ado, which contributes to AdoR activation causing HD pathogenesis, seems to be intracellular and it is mainly released out of the cells through ENT2.

AMPK is not involved in *Drosophila* HD pathogenesis

AMP-activated protein kinase (AMPK) is one of the key enzymes maintaining energy balance within a cell by adjusting anabolic and catabolic pathways (Aymerich, Foufelle, Ferre, Casado, & Pastor-Anglada, 2006); both Ado receptors and transporters have been implicated in its activation (Dolinar, Jan, Pavlin, Chibalin, & Pirkmajer, 2018; Liu et al., 2018; Medina-Pulido et al., 2013; Ruan et al., 2018). Activation of AMPK is beneficial at early stages in mammalian HD models (Vazquez-Manrique et al., 2016); however, in the late stage of the disease it may worsen neuropathological and behavioral phenotypes (Ju et al., 2011).

To find out whether the above-described effects of e-Ado signaling and transport on HD flies are mediated by AMPK (Fig. 4C&D), we co-expressed *Q93 mHTT* with three different recombinant forms of AMPK α subunit(Johnson et al., 2010; Swick, Kazgan, Onyenwoke, & Brenman, 2013), including wild-type AMPKα [M], a phosphomimetic-activated form of AMPKα [T184D], and dominant negative AMPK [DN], and assessed the survival of HD flies. The results showed that neither the activation nor the inhibition of AMPK signaling influenced the eclosion rate (Fig. 4E) or lifespan (Fig. 4F).

To further confirm the genetic data related to AMPK activation or inhibition, we pharmaceutically inhibited AMPK signaling by feeding the larvae with AMPK inhibitor, dorsomorphin (Compound C) (Braco, Gillespie, Alberto, Brenman, & Johnson, 2012). The results showed that although dorsomorphin had an effect on the development of larvae expressing normal Q20 HTT, it did not influence the eclosion of Q93-expressing larvae (Fig. 4G). Overall, our results show that, unlike in mammalian HD models, AMPK signaling does not play a significant role in the pathological manifestations of mHTT in *Drosophila*.

Identification of potential downstream targets of the AdoR/ENT2 pathway by microarray analysis

Our above results indicate that ENT2 and AdoR contribute to mHTT pathogenesis in HD *Drosophila* and work in the same pathway. To identify their downstream target genes, we compared the expression profiles of larvae carrying mutations in *adoR* or *ent2* as well as adult *adoR* mutants using microarrays (Affymetrix), shown as a Venn diagram in Fig. 5A and B. The intersection between each mutant contains differentially expressed transcripts in all three data sets, including six upregulated (Fig. 6A) and seven downregulated mRNAs (Fig. 5B). Interestingly, according to Flybase (http://flybase.org), four of these genes were expressed in the nervous system (*ptp99A* was upregulated, while *CG6184*, *cindr*, and *mod(mdg4)* were downregulated) (Fig. 5C).

To validate the microarray data, we knocked down *adoR* expression in the brain and examined the transcription of the four candidate genes expressed in the nervous system by qPCR. The results revealed that *ptp99A* and *mod(mdg4)* had the same expression trends as observed in the microarrays (Fig. 5D). We further examined whether the expression of *ptp99A* and *mod(mdg4)* are influenced by an increase of e-Ado level. As shown in Fig. 6E, Ado microinjection significantly increased *mod(mdg4)* expression and decreased *ptp99A* expression, confirming that *mod(mdg4)* is positively regulated and *ptp99A* is negatively regulated by the AdoR/ENT2 pathway.

Suppression of *mod(mdg4)* decreased mHTT aggregation and increased survival of HD flies

In order to examine the potential roles of *ptp99A*, *CG6184*, *cindr*, and *mod(mdg4)* genes in HD pathogenesis, we used RNAi to silence them in HD flies. The results showed that only the RNAi silencing of *mod(mdg4)* extended their lifespan. As shown in Figure 6A, the survival curve of HD flies with a silenced *mod(mdg4)* gene was almost identical to the curve specific for *adoR* RNAi HD flies; this effect was stronger than in *ent2* RNAi HD flies. In addition, *mod(mdg4)* RNAi significantly decreased the formation of mHTT inclusions (Fig. 6B&C) and suppressed retinal pigment cell degeneration (Fig. 7D). In contrast to *mod(mdg4)*, RNAi silencing of the other three genes did not show any significant effect.

To further confirm that *mod(mdg4)* is downstream target of the AdoR pathway and regulated by e-Ado signaling, we first checked the expression of *mod(mdg4)* in larval brains and adult heads of HD flies using qPCR. In Q93 larvae, we found that both the expression level of *mod(mdg4)* (Fig. 7A) and the e-Ado level was lower than in Q20-expressing controls (Fig. 1A). For the 15-day-old (roughly corresponding to late-stage HD) Q93 adults, there was no difference in *mod(mdg4)* expression compared to Q20 control adults (Fig. 7A). We next examined the epistasis relationship between *ent2*, *adoR*, and *mod(mdg4)* by combining overexpression of *ent2* or *adoR mod(mdg4)* RNAi in Q93-expressing flies. The results showed that *mod(mdg4)* RNAi suppressed the lethal effects caused by the overexpression of *ent2* and *adoR* (Fig. 8B). These results indicate that *mod(mdg4)* serves as a downstream target of AdoR signaling involved in the process of mHTT inclusion formation and other pathogenic effects (Fig. 7C).

The *mod(mdg4)* locus of *Drosophila* contains several transcription units encoded on both DNA strands producing 31 splicing isoforms(Yu, Waldholm, Bohm, & Visa, 2014). As shown in Fig. 5B, two of the *mod(mdg4)*-specific microarray probes which target 11 *mod(mdg4)* splicing isoforms (Tab. S2) were downregulated in all three datasets. We performed splice form-specific qPCR analysis and found that *adoR* RNAi silencing leads to the downregulation of multiple *mod(mdg4)* isoforms (Fig. 7D), suggesting that AdoR signaling regulates multiple isoforms.

Discussion

Considerable dysregulation of Ado homeostasis has been observed in HD human patients and mice, but the mechanisms of such changes related to HD pathogenesis still need to be characterized(D. Blum et al., 2018). The present study examined the e-Ado titer in the hemolymph of HD *Drosophila* larvae and found that it is lower in Q93-expressing larvae (Fig. 1). Although we did not measure the e-Ado titer in adult flies (due to a problem in acquiring a sufficient amount of hemolymph), the dynamic changes in expression levels of genes involved in Ado homeostasis (Fig. 1D-E), as well as the AdoR-regulated gene, *mod(mdg4)* (Fig. 8A), indicated that e-Ado titer and AdoR activity are variable in different stages of HD. Such dynamic changes of e-Ado homeostasis have also been observed in

rodent HD models, whereby striatal adenosine tone is lower during the early stage of the disease and increased during the later stages(Gianfriddo, Melani, Turchi, Giovannini, & Pedata, 2004; Guitart et al., 2016).

Both the activation and inhibition of $A_{2A}R$ by pharmacological treatments have shown benefits in mammalian HD models. In R6/2 mice, the beneficial effect of activating $A_{2A}R$ is thought to occur *via* the inhibition of AMPK nuclear translocation (which contributes to HD pathogenesis including brain atrophy, neuron death, and increased mHTT aggregates formation) (Ju et al., 2011). Beneficial effects by antagonizing $A_{2A}R$ with SCH58261 in R6/2 mice include reduced striatal glutamate and adenosine outflow as well as restoring emotional behavior and susceptibility to NMDA toxicity (Domenici et al., 2007; Gianfriddo et al., 2004). A_1R activation has also been shown to have neuroprotective effects; however, the chronic administration of A_1R agonists (leading to a desensitisation of A1 receptors) increases neuronal loss whereas the chronic administration of A_1R antagonists (inducing an upregulation of A1 receptors) improves survival and neuronal preservation in the same model (D. Blum, R. Hourez, M. C. Galas, P. Popoli, & S. N. Schiffmann, 2003). Our results show that the genetic depletion of AdoR has beneficial effects on HD flies, while the activation of AdoR contributes to mHTT pathogenesis and aggregates formation.

We observed a non-additive interaction between AdoR and ENT2 characteristic for epistasis relationship (Fig. 4B), indicating that ENT2 is required for the transportation of Ado from the intra- to extracellular environment which activates AdoR and, in turn, enhances the effects of mHTT. Our previous report showed that both ENT2 and AdoR participate in modulating synaptic transmission, and that both *adoR* and *ent2* mutations cause defects in associative learning in *Drosophila*(Knight et al., 2010). Consistently, both the inhibition of Ado release by the knockdown of *ent2* in hemocytes and the mutation of *adoR* suppress metabolic reprogramming and hemocyte differentiation upon immune challenges(Bajgar et al., 2015). Furthermore, another report showed that the disruption of epithelial integrity by Scribbled (*Scrib*) RNAi stimulates Ado release through ENT2, subsequently activating AdoR that, in turn, upregulates tumor necrosis factor (TNF) production which activates JNK signaling(Poernbacher & Vincent, 2018). Interestingly,

while the effects of *ent2* and *adoR* RNAi in HD flies were found to completely overlap, *ent1* RNAi showed a synergistic effect, suggesting potential AdoR-independent mechanisms (Fig. 4A). These results correspond to our previous report showing that *Drosophila* ENT1 has lower specificity for Ado transportation in comparison to ENT2(Fleischmannova et al., 2012). The altered expression of *ent1*, as well as the RNAi effect in HD flies, might be associated with the disturbance of nucleotide homeostasis, similar to that observed in R6/2 and Hdh^{Q150} mice(Toczek et al., 2016).

We identified a downstream target of the AdoR pathway, mod(mdg4), which contributes to the effects of mHTT in the *Drosophila* HD model. The *mod(mdg4)* gene has previously been implicated in the regulation of position effect variegation, chromatin structure, and neurodevelopment(Dorn & Krauss, 2003). The altered expression of *mod(mdg4)* has also been observed in flies expressing untranslated RNA containing CAG and CUG repeats(Mutsuddi, Marshall, Benzow, Koob, & Rebay, 2004; van Eyk et al., 2011). In addition, *mod(mdg4*) has complex splicing, including *trans*-splicing, producing at least 31 isoforms(Krauss & Dorn, 2004). All isoforms contain a common N-terminal BTB/POZ domain which mediates the formation of homomeric, heteromeric, and oligomeric protein complexes(Albagli, Dhordain, Deweindt, Lecocq, & Leprince, 1995; Bardwell & Treisman, 1994; Espinas et al., 1999). Among these isoforms, only two [including *mod(mdg4)*-56.3 (isoform H) and *mod(mdg4)*-67.2 (isoform T)] have been functionally characterized. *Mod(mdg4)*-56.3 is required during meiosis for maintaining the chromosome pairing and segregation in males(Soltani-Bejnood et al., 2007; Thomas et al., 2005). Mod(mdg4)-67.2 interacts with Suppressor of hairy wing [Su(Hw)] and Centrosomal protein 190 kD (CP190) forming a chromatin insulator complex which inhibits the action of the enhancer on the promoter, and is important for early embryo development and oogenesis(Buchner et al., 2000; Melnikova, Kostyuchenko, Parshikov, Georgiev, & Golovnin, 2018; Soshnev, Baxley, Manak, Tan, & Geyer, 2013). Although our results showed that silencing all *mod(mdg4)* isoforms decreases the effects of mHTT (Fig. 6), we could not clarify which of the isoforms is specifically involved in HD pathogenesis because AdoR signaling regulates multiple isoforms (Fig. 7D). Interestingly, an earlier report on protein two-hybrid screening indicated that Mod(mdg4) interacts with six Hsp70 family proteins(Giot et al., 2003; Oughtred et al., 2019), and Hsp70 proteins are

known for their contribution to the suppression of polyQ aggregates formation and neurodegeneration (Chan, Warrick, Gray-Board, Paulson, & Bonini, 2000; Warrick et al., 1999). Further study will be needed to identify the specific *mod(mdg4)* isoform involved in HD pathogenesis, and whether a decrease in mHTT aggregates by mod(mdg4) RNAi is connected to Hsp70 interaction.

In summary, we observed an alteration in the e-Ado concentration and expression of genes involved in Ado homeostasis in a *Drosophila* HD model. By candidate RNAi screening, we demonstrated that the silencing of *ent2* and *adoR* increases the survival of HD flies in addition to suppressing retinal cell degeneration and mHTT aggregate formation. We also showed that the activation of e-Ado signaling enhances the effects of mHTT. Furthermore, we found that *mod(mdg4)* is a downstream target of the AdoR pathway and plays a major role in the pathogenesis of HD flies. Our work enhances our understanding of e-Ado signaling in HD pathogenesis and may open up new opportunities for HD pharmacological intervention.

Materials and methods

Fly stocks

Flies were reared at 25 °C on standard cornmeal medium. The following RNAi lines were acquired from the TRiP collection (Transgenic RNAi project) at Harvard Medical School: adgfA-Ri (BL67233), adgfC-Ri (BL42915), adgfD-Ri (BL56980), adenoK-Ri (BL64491), ent1-Ri (BL51055), adoR-Ri (BL27536), gfp-Ri (BL41552), mod(mdg4)-Ri (BL32995), cindr-Ri (BL38976), and ptp99A-Ri (BL57299). The following RNAi lines were acquired from the Vienna Drosophila RNAi Center (VDRC): ent2-Ri (ID100464), ent3-Ri (ID47536), cnt2-Ri (ID37161), and cg6184-Ri (ID107150). The following lines were provided by the Bloomington Drosophila Stock Center: UAS-AMPKα^{T184D} (BL32110), UAS-AMPKα^{M} (BL32108), UAS-AMPKα^{DN} (AMPKα^{K57A}, BL32112), and elav^{C155}-GAL4 (BL458).

Flies overexpressing human normal huntingtin (HTT) exon 1, Q20Httexon^{1111F1L} or mutant pathogenic fragments (mHTT), Q93Httexon^{14F132} were obtained from Prof. Lawrence

Marsh (UC Irvine, USA)(Steffan et al., 2001). The UAS-overexpression lines, Ox-adenoK and Ox-adoR (s), were obtained from Dr. Ingrid Poernbacher (The Francis Crick Institute, UK)(Poernbacher & Vincent, 2018). gmr-GAL4 was obtained from Dr. Marek Jindra (Biology Centre CAS, Czechia). da-GAL4 was obtained from Dr. Ulrich Theopold (Stockholm University). The UAS overexpression strains Ox-adgfA, Ox-ent2, and Ox-adoR (w), as well as $adoR^{1}$ and $ent2^{3}$ mutant flies, were generated in our previous studies(Dolezal, Dolezelova, Zurovec, & Bryant, 2005; Dolezal, Gazi, Zurovec, & Bryant, 2003; Dolezelova, Nothacker, Civelli, Bryant, & Zurovec, 2007; Knight et al., 2010).

Eclosion rate and adult lifespan assay

For assessing the eclosion rate, male flies containing the desired RNAi or overexpression transgene (RiOx) in the second chromosome with genotype w^{1118}/Y; RiOx /CyO; UAS-Q93/MKRS were crossed with females of *elav-GAL4*; +/+; +/+. The ratio of eclosed adults between *elav-GAL4*/+; RiOx/+; UAS-Q93/+ and *elav-GAL4*/+; RiOx/+; +/MKRS was then calculated. If the desired RiOx transgene was in the third chromosome, female flies containing *elav-GAL4*; +/+; RiOx were crossed with male w^{1118}/Y; +/+; UAS-Q93/MKRS, and the ratio of eclosed adults between *elav-GAL4*; +/+; RiOx/UAS-Q93 and *elav-GAL4*; +/+; RiOx/MKRS was calculated.

For the adult lifespan assay, up to 30 newly emerged female adults were placed in each cornmeal vial and maintained at 25 ℃. At least 200 flies of each genotype were tested, and the number of dead flies was counted every day. Flies co-expressing RiOx and Q20 were used for evaluating the effect of RNAi or overexpression of the desired transgenes (Fig. S3A&B).

Extracellular adenosine and ATP level measurements

To collect the hemolymph, six third instar larvae (96 hours post-oviposition) were torn in 150 µl of 1× PBS containing thiourea (0.1 mg/ml) to prevent melanization. The samples were then centrifuged at 5000× *g* for 5 min to separate the hemocytes and the supernatant was collected for measuring the extracellular adenosine or ATP level. For measuring the adenosine titer, 10 µl of hemolymph was mixed with reagents of an adenosine assay kit

(Biovision) following the manufacturer's instructions. The fluorescent intensity was then quantified (Ex/Em = 533/ 587 nm) using a microplate reader (BioTek Synergy 4). For measuring the ATP level, 10 µl of hemolymph was incubated with 50 µl of CellTiter-Glo reagent (Promega) for 10 min. Then, the luminescent intensity was quantified using an Orion II microplate luminometer (Berthold). To calibrate the standard curve of ATP concentration, 25 µM ATP standard solution (Epicentre) was used for preparing a concentration gradient (0, 2, 4, 6, 8, 10 µM) of ATP solution and the luminescent intensity was measured for each concentration. The protein concentration of the hemolymph sample was determined by A280 absorbance using a NanoDrop 2000 spectrophotometer (Thermo Fisher). The adenosine and ATP concentrations were first normalized to protein concentration. Then, the values of Q20 and Q93 samples were normalized to values of the *GAL4* control sample. Six independent replicates for each genotype were performed for the analysis of adenosine and ATP levels.

RNA extraction

The brains from 10 third-instar larvae (96 hours post-oviposition), heads from 30 female adults (5 days or 15 days old) or 15 whole female flies were collected. The samples were first homogenized in RiboZol (VWR) and the RNA phase was separated by chloroform. For brain or head samples, the RNA was precipitated by isopropanol, washed in 75% ethanol and dissolved in nuclease-free water. For whole fly samples, the RNA phase was purified using NucleoSpin RNA columns (Macherey-Nagel) following the manufacturer's instructions. All purified RNA samples were treated with DNase to prevent genomic DNA contamination. cDNA was synthesized from 2 µg of total RNA using a RevertAid H Minus First Strand cDNA Synthesis Kit (Thermo Fisher Scientific).

Adenosine injection

Three- to five-day-old female adults were injected with 50 nl of 10 mM adenosine using a NANOJECT II (Drummond Scientific); control flies were injected with 50 nl of 1× PBS. Two hours post-injection, 15 injected flies for each replicate were collected for RNA extraction.

Microarray analysis

The Affymetrix GeneChip® *Drosophila* genome 2.0 array system was used for microarray analysis following the standard protocol: 100 ng of RNA was amplified with a GeneChip 3′ express kit (Affymetrix), and 10 μg of labeled cRNA was hybridized to the chip according to the manufacturer's instructions. Statistical analysis of array data were described previously in our studies(Arefin et al., 2014; Kucerova et al., 2016). Storey's q value (false discovery rate, FDR) was used to select significantly differentially transcribed genes ($q < 0.05$). Transcription raw data are shown in Table S2. The transcription data are deposited in the ArrayExpress database (www.ebi.ac.uk/arrayexpress; accession No. E-MTAB-8699 and E-MTAB-8704).

qPCR and primers

5× HOT FIREPol® EvaGreen® qPCR Mix Plus with ROX (Solis Biodyne) and an Eco Real-Time PCR System (Illumina) were used for qPCR. Each reaction contained 4 μl of EvaGreen qPCR mix, 0.5 μl each of forward and reverse primers (10 μM), 5 μl of diluted cDNA and ddH2O to adjust the total volume to 20 μl. The list of primers is shown in Table S1. The expression level was calculated using the $2^{-\Delta\Delta Ct}$ method. The ct values of target genes were normalized to reference gene, ribosomal protein 49 (*rp49*).

Imaging of retinal pigment cell degeneration

Twenty- and thirty-day-old female adults were collected and their eye depigmentation phenotypes were recorded. At least 30 individuals for each genotype were examined under a microscope, and at least five representative individuals were chosen for imaging. Pictures were taken with an EOS 550D camera (Canon) mounted on a SteREO Discovery V8 microscope (Zeiss).

Immunostaining

Brains dissected from 10- or 20-day-old adult females were used for immunostaining. The brains were fixed in 4% PFA, permeabilized with PBST (0.1% Triton X-100), blocked in PAT (PBS, 0.1% Triton X-100, 1% BSA) and stained with antibodies in PBT (PBS, 0.3% Triton X-100, 0.1% BSA). Primary antibodies used in this study were mouse anti-HTT,

MW8 which specifically binds to mHTT aggregates (1:40, DSHB), and rat anti-Elav (1:40, DSHB) which is a pan-neuronal antibody. Secondary antibodies were Alexa Fluor 488 anti-mouse and Alexa Fluor 647 anti-rat (1:200, Invitrogen). The samples were mounted in Fluoromount-G (Thermo Fisher) overnight, prior to image examination.

Quantification of mHTT aggregates

Images of aggregates were taken using a Flowview 100 confocal microscope (Olympus). The intensity of mHTT aggregates detected by anti-HTT antibody (MW8) or anti-Elav were quantified using ImageJ software. The level of mHTT aggregates was quantified by normalizing the mHTT aggregates intensity to Elav intensity. At least six brain images from each genotype were analyzed.

AMPK inhibitor (dorsomorphin) feeding

Thirty first instar of Q20- or Q93-exexpressing larvae were collected for each replicate 24 hours after egg laying. Larvae were transferred to fresh vials with 0.5 g instant *Drosophila* medium (Formula 4–24, Carolina Biological Supply, Burlington, NC) supplemented with 2 mL distilled water containing either dorsomorphin (100 μM) or DMSO (1%). Total number of emerging adults were counted.

Statistical analysis

Error bars show standard error of the mean throughout this paper. Significance was established using Student's t-test (N.S., not significant; * $P < 0.05$, ** $P < 0.01$, *** $P < 0.001$) or one-way ANOVA analysis with Tukey's HSD *post-hoc* test. For the statistical analysis of survival curves, we used the online tool OASIS 2 to perform a weighted log-rank test (Wilcoxon-Breslow-Gehan test) for determining significance(Han et al., 2016).

Figures

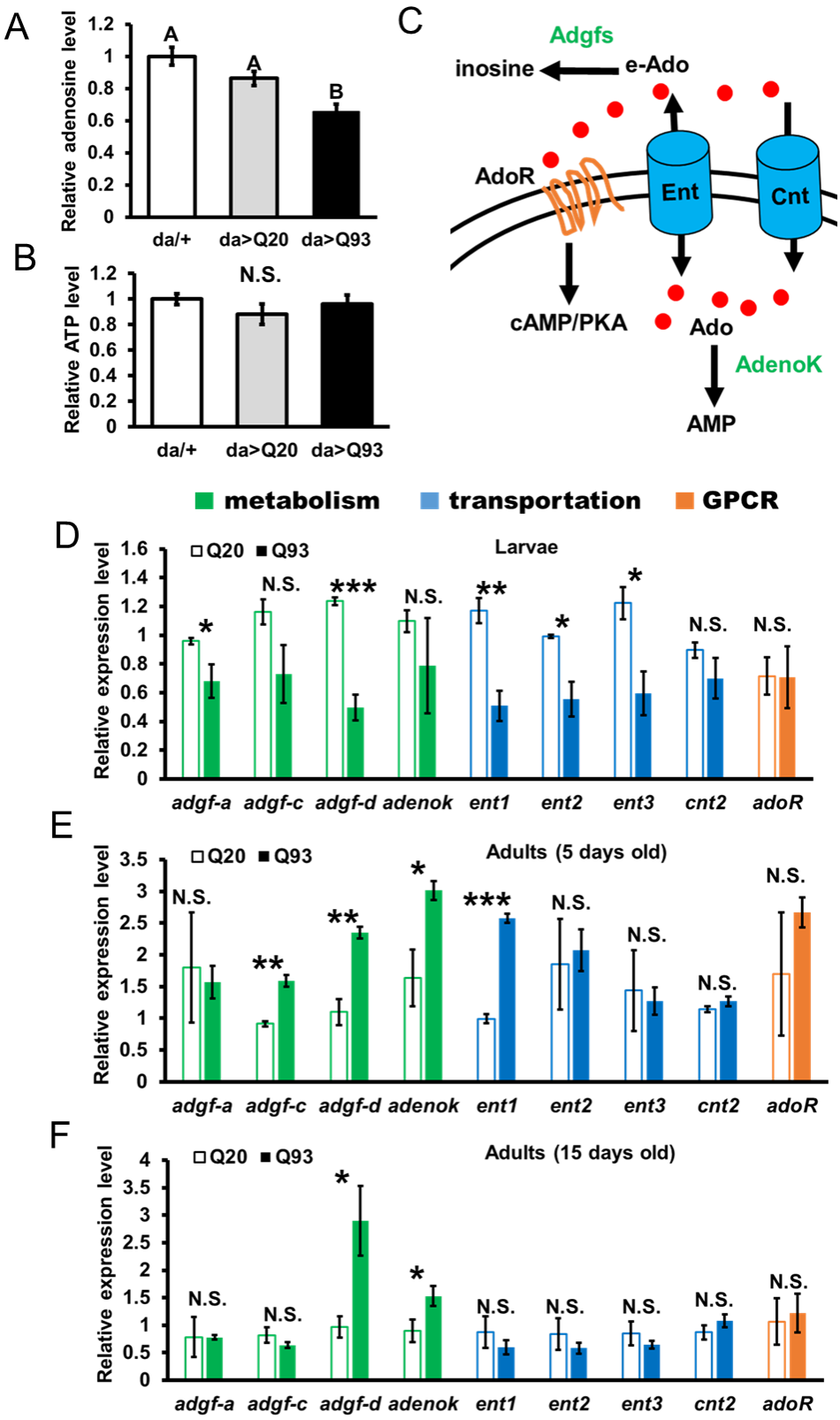

506

Figure 1. Alteration of adenosine homeostasis in the *Drosophila* HD model. (A-B) The measurements of extracellular adenosine levels (A) and extracellular ATP levels (B) in Q93-expressing (da>Q93), Q20-expressing (da>Q20) and control *da*-GAL4 (da/+) larvae. Six independent replicates were measured. Significance was analyzed by ANOVA with Tukey's HSD *post-hoc* test; significant differences ($P < 0.05$) among treatment groups are marked with different letters. (C) Diagram showing the interaction of adenosine metabolic enzymes, transporters, and receptors in *Drosophila*. (D-F) Expression profiles of genes involved in adenosine metabolism (green) and adenosine transportation (blue) as well as adenosine receptors (orange) at different stages in HD *Drosophila* brains (larvae) or heads (adults). The expression of Q20 and Q93 were driven by the pan-neuronal driver (*elav*-GAL4). Three independent replicates were measured. The significances of results were examined using Student's t-test: $*P < 0.05$, $**P < 0.01$, $***P < 0.001$; N.S., not significant. All data are presented as mean ± SEM

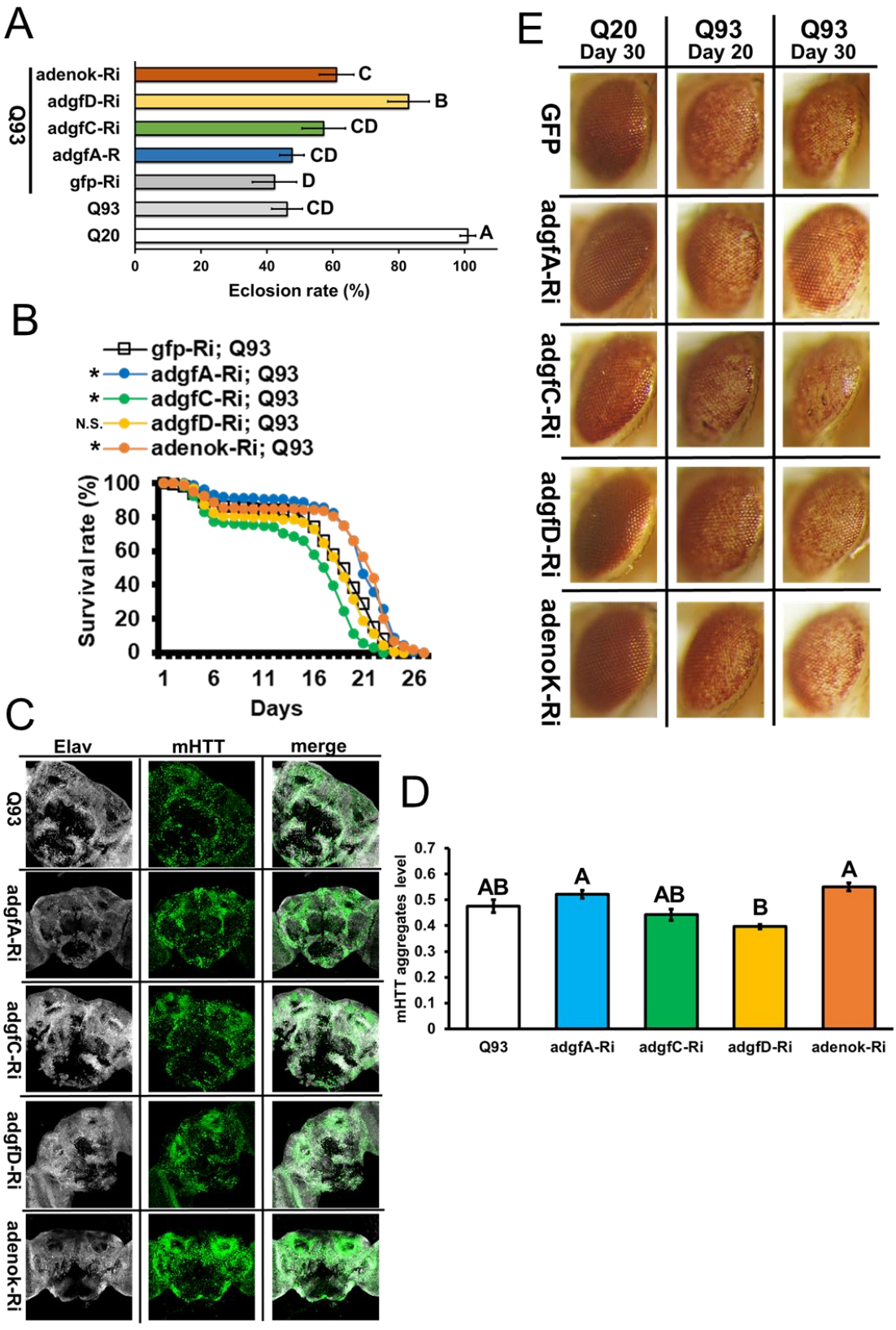

533

534

Figure 2. RNAi-mediated (Ri) downregulation of adenosine metabolic genes in HD *Drosophila*. Co-expression Q93 with each RNAi transgenes were driven by the pan-neuronal driver, *elav*-GAL4 (A-D), or eye driver, *gmr-GAL4* (E). The adult eclosion rate (A), adult lifespan (B), mHTT aggregate levels (C-D), and retinal pigment cell degeneration (E) were compared. † Eye image of homozygous *adoR*^{1} mutant without *htt* expression. At least five independent replicates were measured for eclosion rate. Detailed methodologies of the lifespan assay, eye imaging, and quantification of mHTT aggregates are described in Materials and methods. Significance values of the eclosion rate (A) and mHTT aggregates levels (D) were analyzed by ANOVA with Tukey's HSD *post-hoc* test; significant differences ($P < 0.05$) among treatment groups are marked with different letters. Significance values for the adult lifespan curve (B) were analyzed by a weighted log-rank test, and significant differences between control gfp-Ri flies with each RNAi group are labeled as follows: *$P < 0.05$; N.S., not significant. Error bars are presented as mean ± SEM

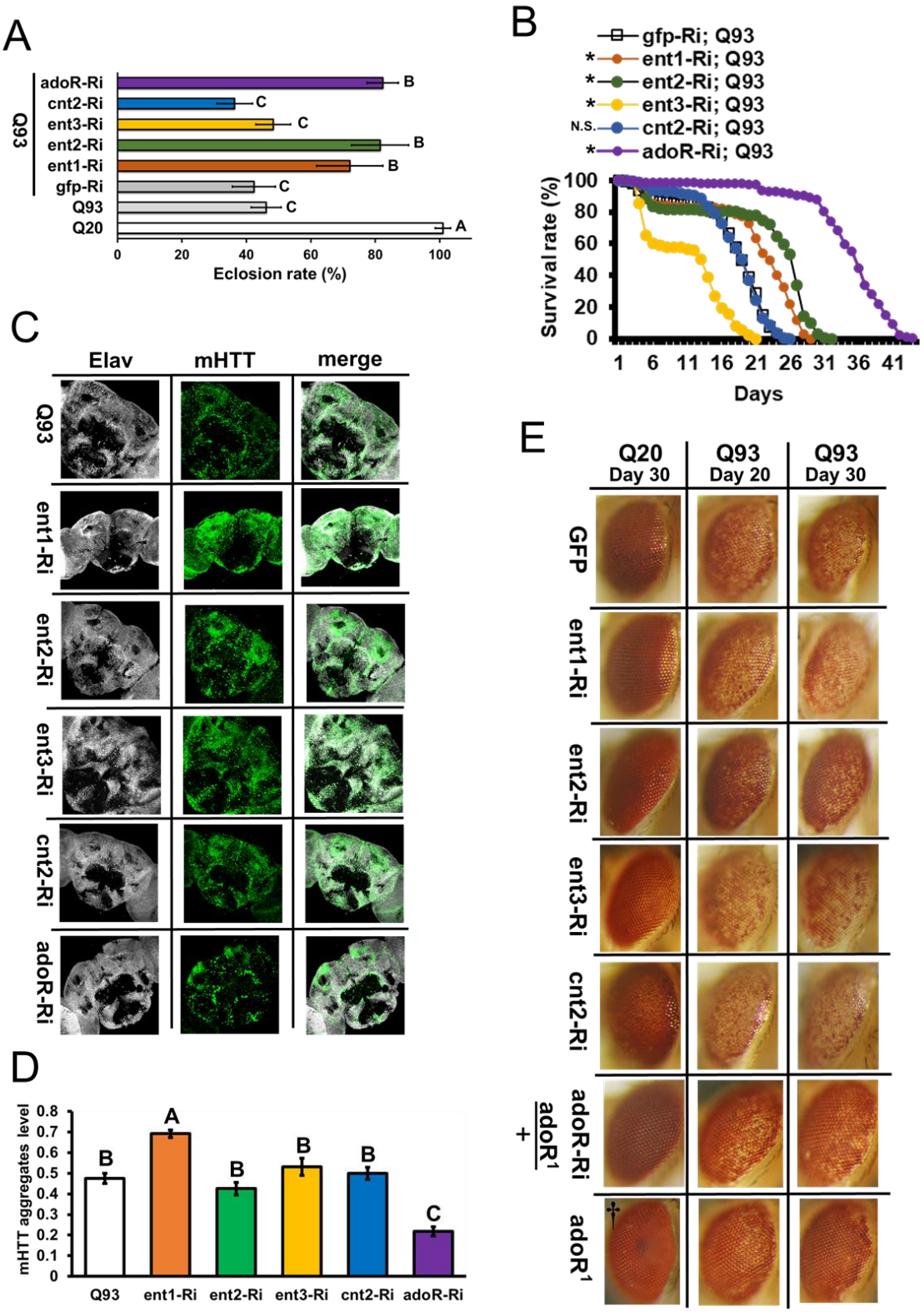

561

562

Figure 3. RNAi-mediated (Ri) downregulation of adenosine transporters and adenosine receptor (*adoR*) in HD *Drosophila*. Co-expression of Q93 with each RNAi transgene was driven by the pan-neuronal driver, *elav*-GAL4 (A-D), or eye driver, *gmr*-GAL4 (E). The adult eclosion rate (A), adult lifespan (B), mHTT aggregate levels (C-D), and retinal pigment cell degeneration (E) were compared. At least five independent replicates were measured for eclosion rate. Detailed methodologies of the lifespan assay, eye imaging, and quantification of mHTT aggregates are described in Materials and methods. Significance values for eclosion rate (A) and mHTT aggregates levels (D) were analyzed by ANOVA with Tukey's HSD *post-hoc* test; significant differences ($P < 0.05$) among treatment groups are marked with different letters. Significance values for the adult lifespan curve (B) were analyzed by a weighted log-rank test; significant differences comparing control gfp-Ri with each RNAi group are labeled as follows: $*P < 0.05$; N.S., not significant. Error bar are presented as mean ± SEM

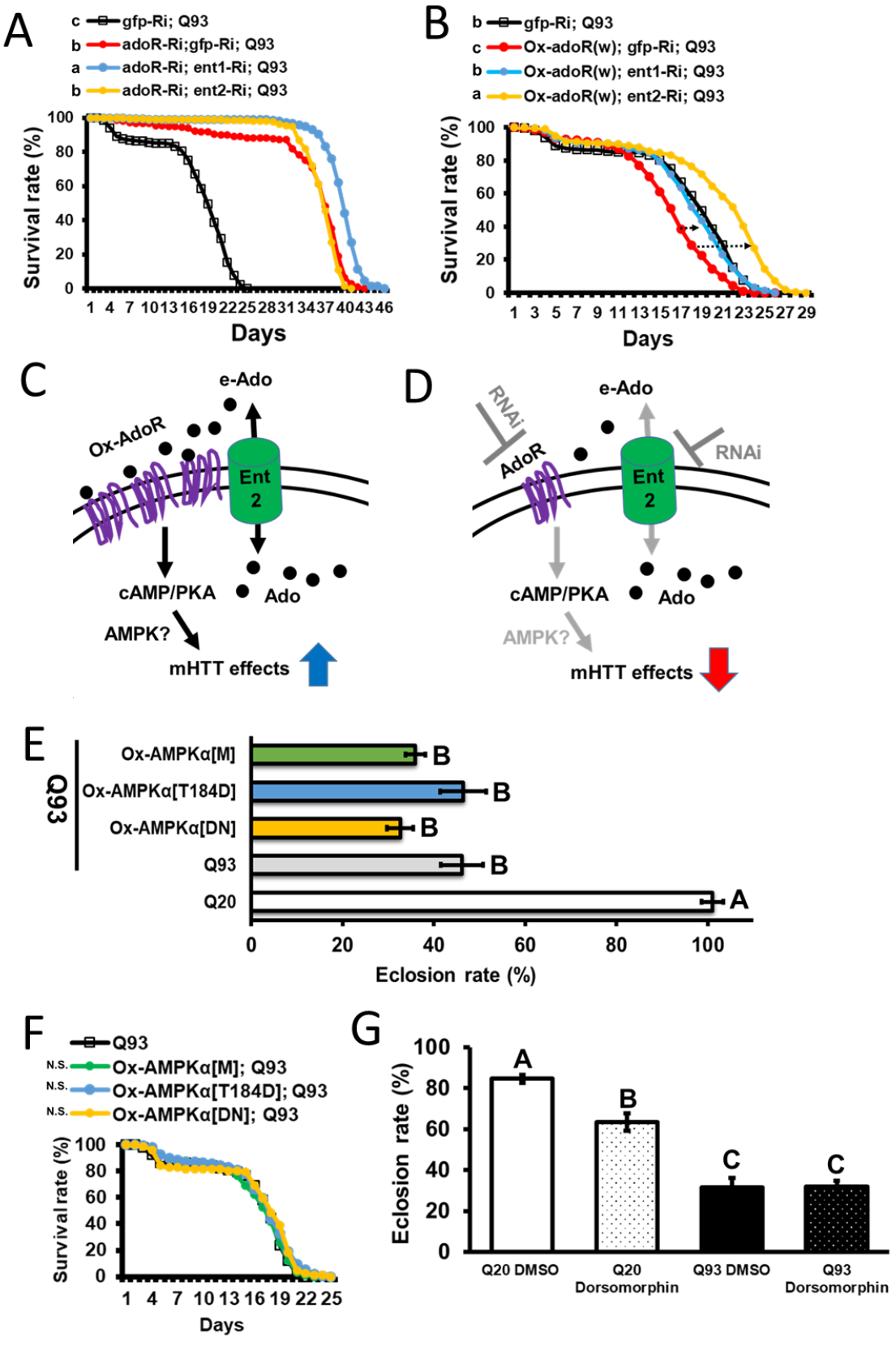

589

Figure 4. Interactions of AdoR and ENTs as well as the impacts of AMPK activity in HD *Drosophila*. (A) Co-expression of *adoR* RNAi with *ent1* or *ent2* RNAi in HD flies. (B) Co-expression of *adoR* overexpressing construct (Ox-adoR) with *ent1* or *ent2* RNAi transgenes in HD flies. (C-D) Diagrams showing the action of Ado in mHTT pathogenesis. Co-expression of Q93 with overexpression of wild-type AMPKα [M], phosphomimetic-activated form of AMPKα [T184D], and dominant negative AMPK [DN] were driven by the pan-neuronal driver (*elav*-GAL4); the adult eclosion rate (E) and survival curve (F) were compared. (G) Q20- and Q93-expressing larvae were fed with AMPK inhibitor, dorsomorphin, or control DMSO, and the adult eclosion rates were assessed. Significance values of the adult lifespan curve were analyzed by a weighted log-rank test; different letters indicate significant differences ($P < 0.05$) among treatment groups. N.S., not significant. Significance values of (E) and (G) were analyzed by ANOVA with Tukey's HSD *post-hoc* test; significant differences ($P < 0.05$) among treatment groups are marked with different letters.

A

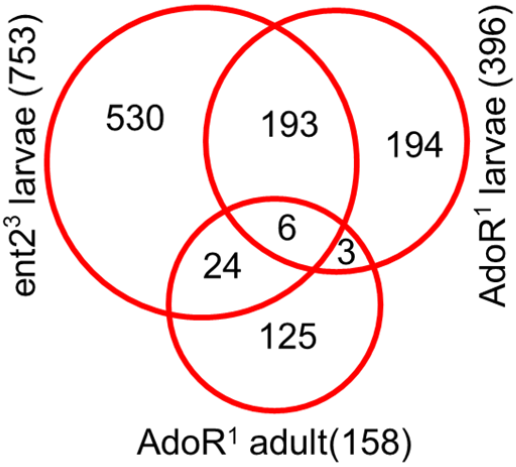

B

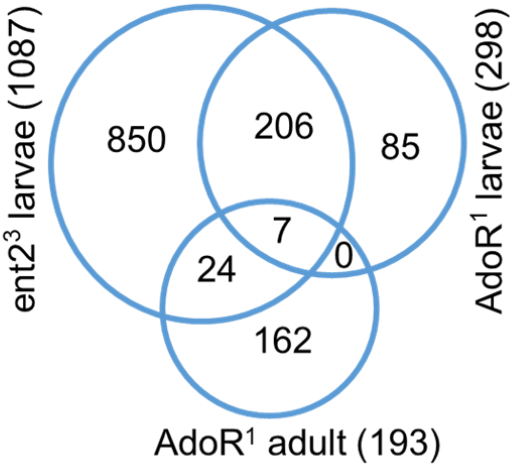

C

Probe ID	gene	CG	Log fold change Ent2³-L	AdoR¹-L	AdoR¹-A	Localization
1641190_at	Jon65Aii	CG6580	2.79	2.5	3.18	MG
1627771_at		CG13075	2.58	2.91	1.93	HG, MT
1630590_at		CG18417	2.02	3.48	4.35	MG, HG
1624393_at	w	CG2759	1.77	4.97	4.5	MT
1632003_a_at	Ptp99A	CG11516	1.53	1.41	2.32	ID, NS, T
1632404_at	rtet	CG5760	1.02	0.85	2.09	MG, HG, I
1633369_s_at		CG6184	-0.23	-0.21	-0.68	NS, tes
1637389_at	Ir100a	CG11575	-0.67	-0.68	-2.61	non-spec
1635901_at		CG17197	-0.85	-0.63	-1.09	ID, tes
1624020_at	mod(mdg4)	CG32491	-1	-1.4	-0.57	NS, ID
1640850_at	cindr	CG31012	-1.11	-1.1	-1.02	NS, SS, ID, tes
1627953_at	mod(mdg4)	CG32491	-1.28	-1.08	-1.19	NS, ID
1633748_at	ND-20L	CG2014	-1.94	-2.05	-0.82	ID, tes

D

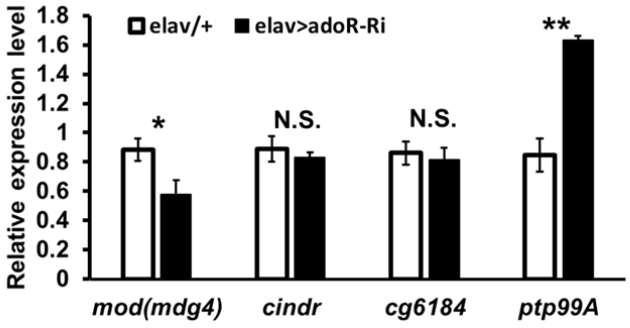

E

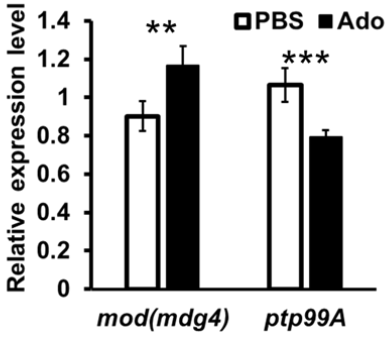

606

Figure 5. Identification of potential downstream targets of AdoR by microarray analysis. (A-B) Venn diagram showing the number of common genes (in intersect region) which are upregulated (A) or downregulated (B) among the *adoR* mutant larvae vs. control (w^{1118}), *adoR* mutant adults vs. control (w^{1118}), and *ent2* mutant larvae vs. control (w^{1118}). The cutoff values for expression differences were set at $Q < 0.05$ (false discovery rate, FDR). (C) The intersection between the three datasets; tissue localization of each gene expression was obtained from Flybase (http://flybase.org/). Tissue abbreviations: midgut (MG), hindgut (HG), Malpighian tubule (MT), imaginal disc (ID), integument (I), sensory system (SS), nervous system (NS), trachea (T), testis (tes), nonspecific expression (non-spec) (D) qPCR confirmed the potential AdoR-regulated genes expressed in the nervous system. Expression of *adoR* RNAi transgenes (adoR-Ri) was driven by the pan-neuronal driver (elav>adoR-Ri), and control flies contained *elav*-GAL4 (elav/+) only. (E) Enhancing extracellular adenosine signaling by adenosine injection and qPCR examination demonstrated that *mod(mdg4)* is positively- and *ptp99A* is negatively-regulated by adenosine signaling. Three independent replicates were measured in qPCR experiments. The qPCR primers of *mod(mdg4)* were selected to target the common 5′ exon shared in all of the isoforms. Student's t-test was used to examine the significance of qPCR results: $*P < 0.05$, $**P < 0.01$, $***P < 0.001$; N.S., not significant. Error bars are presented as averages ± SEM

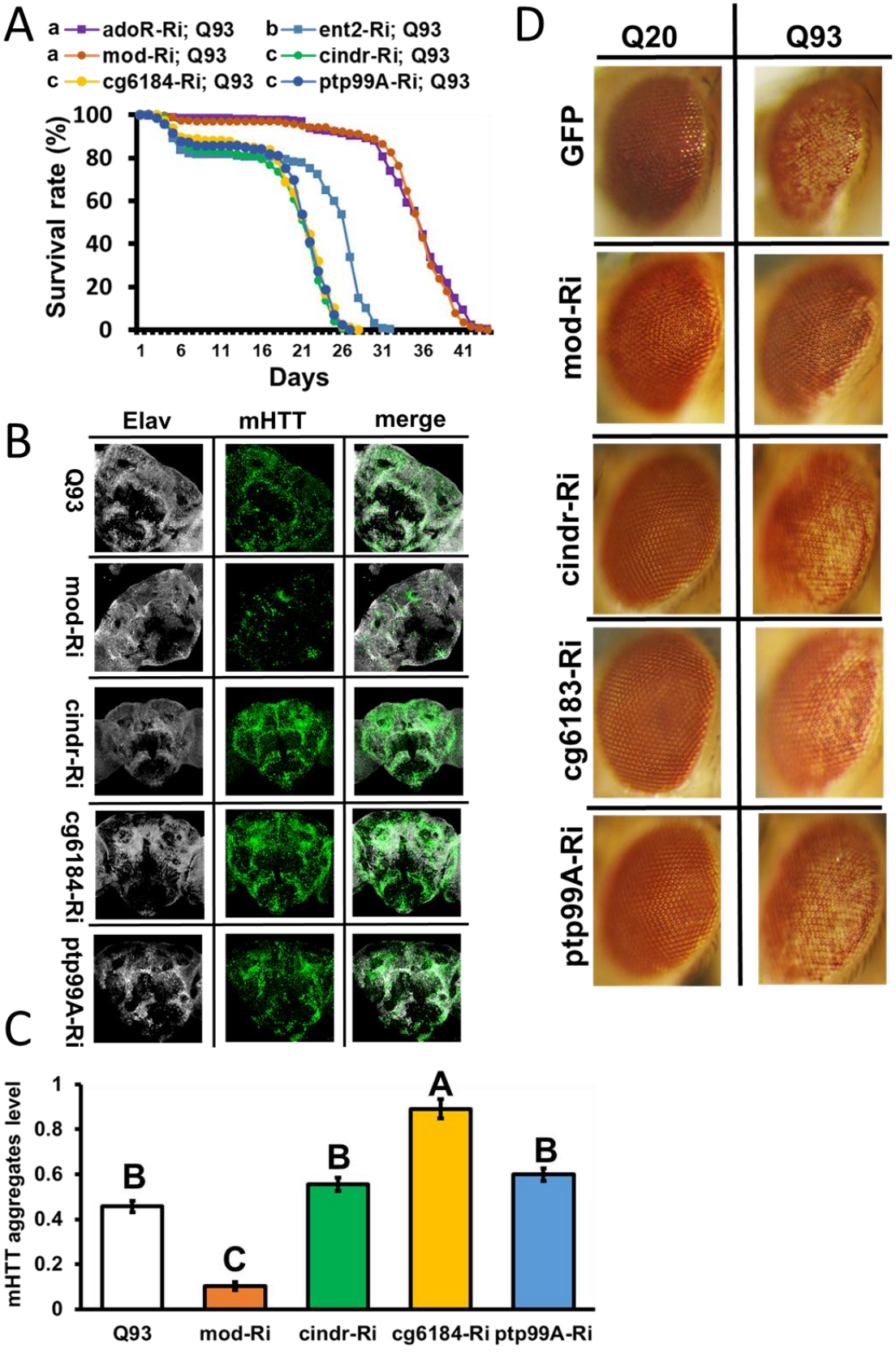

635

Figure 6. RNAi-mediated (Ri) downregulation of potential downstream targets of AdoR signaling in HD *Drosophila*. Co-expression of Q93 with each RNAi transgene, including *ptp99A*, *CG6184*, *cindr*, and *mod(mdg4)*, were driven by the pan-neuronal driver, *elav*-GAL4 (A-B), or the eye driver, *gmr*-GAL4 (D). The adult lifespan (A), mHTT aggregate levels (B-C), and retinal pigment cell degeneration (D) were compared. A detailed methodology of the lifespan assay, eye imaging, and quantification of mHTT aggregates are described in Materials and methods. Significance values of the adult lifespan curve (A) were analyzed by a weighted log-rank test, and different letters indicate significant differences ($P < 0.05$) among treatment groups. Significance values of mHTT aggregate levels (C) were analyzed by ANOVA with Tukey's HSD *post-hoc* test; significant differences ($P < 0.05$) among treatment groups are marked with different letters. Error bars are presented as mean ± SEM

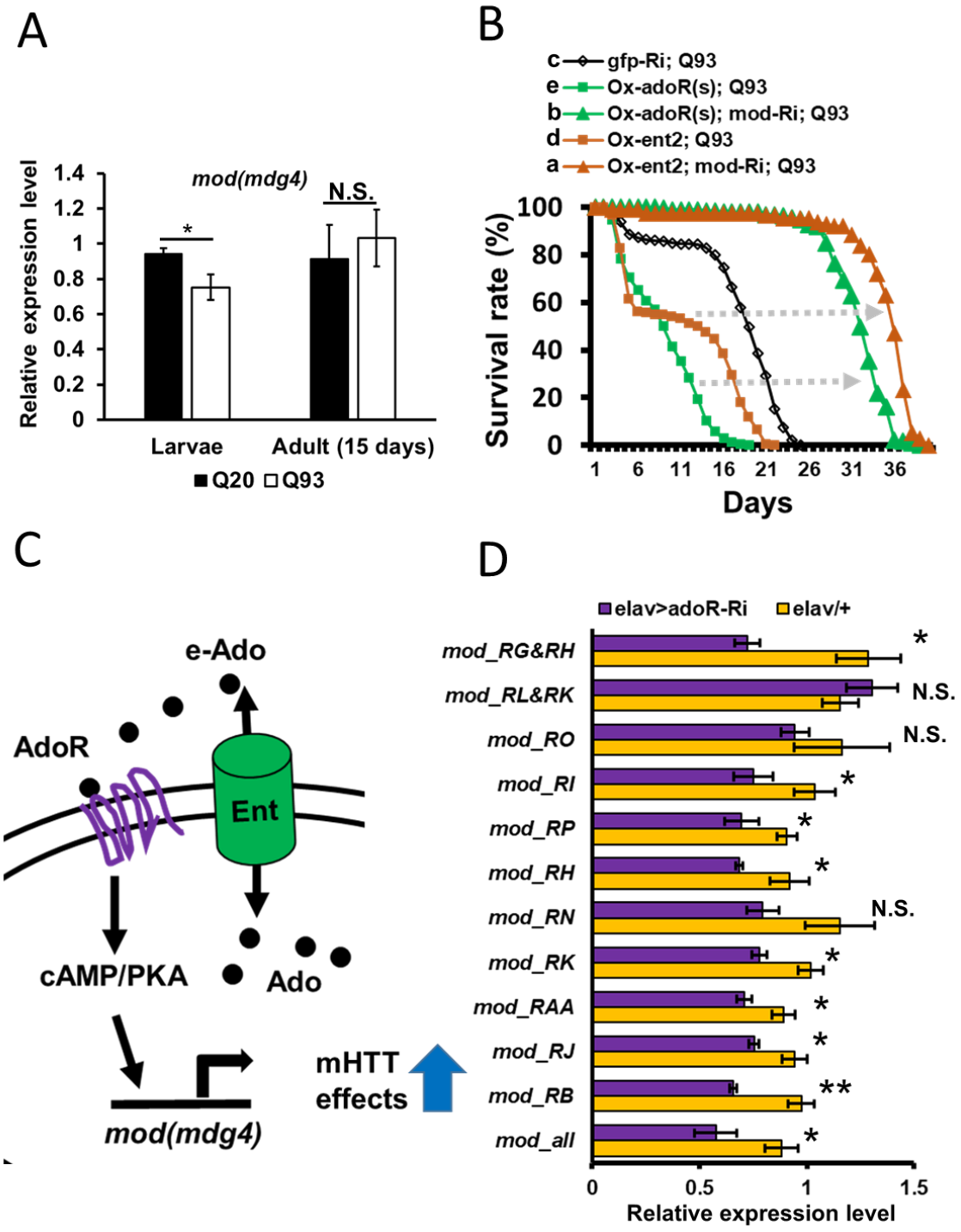

662

663

664

Figure 7. *mod(mdg4)* as a AdoR-regulated gene contributes to HD pathogenesis. (A) qPCR analysis of the expression of *mod(mdg4)* in the larval brain and 15-day-old adult heads of Q20- and Q93-expressing flies. The qPCR primers of *mod(mdg4)* targeted the common 5′ exon shared by all isoforms. (B) Epistasis analysis showed that *ent2* (Ox-ent2) and *adoR* overexpression (Ox-adoR) with *mod(mdg4)* RNAi transgenes in HD flies decreased the mortality effect caused by *ent2* and *adoR* overexpression. This suggests that *mod(mdg4)* is downstream of the AdoR pathway (C). qPCR identified potential *mod(mdg4)* isoforms regulated by the AdoR pathway. *adoR* RNAi transgene (adoR-Ri) expression was driven by the pan-neuronal driver (elav>adoR-Ri); control flies contained only *elav*-GAL*4* (elav/+). Mod_all indicates that the primers targeted all *mod(mdg4)* isoforms. Isoforms L and G do not have their own unique exonal region, therefore it is possible for the qPCR primers to target two isoforms simultaneously (presented as RG&RG and RL&RK). qPCR result significance was examined using Student's t-test: $*P < 0.05$, $**P < 0.01$, $***P < 0.001$; N.S., not significant. Significance values for the adult lifespan curve (A) were analyzed by weighted log-rank test, and different letters indicate significant differences ($P < 0.05$) among treatment groups. Error bars are presented as mean ± SEM

Acknowledgements

We thank Dr. Ingrid Poernbacher (The Francis Crick Institute, UK), Prof. Lawrence Marsh (UC Irvine, USA), Dr. Marek Jindra (Biology Centre CAS, Czechia), Dr. Tomas Dolezal (University of South Bohemia, Czechia), Dr. Ulrich Theopold (Stockholm University), Bloomington *Drosophila* Stock Center and Vienna *Drosophila* Resource Center for providing us with fly strains. This work was supported by the grant agency of the University of South Bohemia (065/2017/P to Y-HL), junior grant project GACR (19-13784Y to LK) and European Community's Programme Interreg Östereich-Tschechische Republik (REGGEN/ATCZ207 to MZ).

Author Contributions

Y-HL performed the experiments and prepared the manuscript. HM assisted in recording the adult lifespan and eye phenotypes as well as performed the brain dissection, immunochemistry and confocal microscopy imaging. LK performed the sample preparation and analyzed the microarray data. LR assisted in recording the adult lifespan, eye phenotype and prepared fly strains. TF established the methodologies for recording the eclosion rate, survival and prepared fly strains. MZ conceived the project and supervised manuscript preparation.

References

Albagli, O., Dhordain, P., Deweindt, C., Lecocq, G., & Leprince, D. (1995). The BTB/POZ domain: a new protein-protein interaction motif common to DNA- and actin-binding proteins. *Cell Growth Differ, 6*(9), 1193-1198.

Anderson, C. M., & Nedergaard, M. (2006). Emerging challenges of assigning P2X7 receptor function and immunoreactivity in neurons. *Trends Neurosci, 29*(5), 257-262. doi:10.1016/j.tins.2006.03.003

Arefin, B., Kucerova, L., Dobes, P., Markus, R., Strnad, H., Wang, Z., . . . Theopold, U. (2014). Genome-wide transcriptional analysis of Drosophila larvae infected by entomopathogenic nematodes shows involvement of complement, recognition and extracellular matrix proteins. *J Innate Immun, 6*(2), 192-204. doi:10.1159/000353734

Aymerich, I., Foufelle, F., Ferre, P., Casado, F. J., & Pastor-Anglada, M. (2006). Extracellular adenosine activates AMP-dependent protein kinase (AMPK). *J Cell Sci, 119*(Pt 8), 1612-1621. doi:10.1242/jcs.02865

725 Bajgar, A., & Dolezal, T. (2018). Extracellular adenosine modulates host-pathogen interactions
726 through regulation of systemic metabolism during immune response in Drosophila. *PLoS*
727 *Pathog, 14*(4), e1007022. doi:10.1371/journal.ppat.1007022
728 Bajgar, A., Kucerova, K., Jonatova, L., Tomcala, A., Schneedorferova, I., Okrouhlik, J., & Dolezal,
729 T. (2015). Extracellular adenosine mediates a systemic metabolic switch during immune
730 response. *PLoS Biol, 13*(4), e1002135. doi:10.1371/journal.pbio.1002135
731 Bardwell, V. J., & Treisman, R. (1994). The POZ domain: a conserved protein-protein interaction
732 motif. *Genes Dev, 8*(14), 1664-1677. doi:10.1101/gad.8.14.1664
733 Blum, D., Chern, E. C., Domenici, M. R., Buée, L., Lin, C. Y., Ferré, S., & Popoli, P. (2018). What Is
734 the Role of Adenosine Tone and Adenosine Receptors in Huntington's Disease? In P. A.
735 Borea, K. Varani, S. Gessi, S. Merighi, & F. Vincenzi (Eds.), *The Adenosine Receptors* (pp.
736 281-308). Cham: Springer International Publishing.
737 Blum, D., Chern, Y., Domenici, M. R., Buee, L., Lin, C. Y., Rea, W., . . . Popoli, P. (2018). The Role
738 of Adenosine Tone and Adenosine Receptors in Huntington's Disease. *J Caffeine*
739 *Adenosine Res, 8*(2), 43-58. doi:10.1089/caff.2018.0006
740 Blum, D., Hourez, R., Galas, M.-C., Popoli, P., & Schiffmann, S. N. (2003). Adenosine receptors
741 and Huntington's disease: implications for pathogenesis and therapeutics. *The Lancet*
742 *Neurology, 2*(6), 366-374. doi:https://doi.org/10.1016/S1474-4422(03)00411-3
743 Blum, D., Hourez, R., Galas, M. C., Popoli, P., & Schiffmann, S. N. (2003). Adenosine receptors
744 and Huntington's disease: implications for pathogenesis and therapeutics. *Lancet*
745 *Neurol, 2*(6), 366-374. doi:10.1016/s1474-4422(03)00411-3
746 Braco, J. T., Gillespie, E. L., Alberto, G. E., Brenman, J. E., & Johnson, E. C. (2012). Energy-
747 dependent modulation of glucagon-like signaling in Drosophila via the AMP-activated
748 protein kinase. *Genetics, 192*(2), 457-466. doi:10.1534/genetics.112.143610
749 Buchner, K., Roth, P., Schotta, G., Krauss, V., Saumweber, H., Reuter, G., & Dorn, R. (2000).
750 Genetic and molecular complexity of the position effect variegation modifier
751 mod(mdg4) in Drosophila. *Genetics, 155*(1), 141-157.
752 Chan, H. Y., Warrick, J. M., Gray-Board, G. L., Paulson, H. L., & Bonini, N. M. (2000). Mechanisms
753 of chaperone suppression of polyglutamine disease: selectivity, synergy and modulation
754 of protein solubility in Drosophila. *Hum Mol Genet, 9*(19), 2811-2820.
755 doi:10.1093/hmg/9.19.2811
756 Cunha, R. A. (2001). Adenosine as a neuromodulator and as a homeostatic regulator in the
757 nervous system: different roles, different sources and different receptors.
758 *Neurochemistry International, 38*(2), 107-125. doi:Doi 10.1016/S0197-0186(00)00034-6
759 Cunha, R. A. (2019). Signaling by adenosine receptors-Homeostatic or allostatic control? *PLoS*
760 *Biol, 17*(4), e3000213. doi:10.1371/journal.pbio.3000213
761 Dolezal, T., Dolezelova, E., Zurovec, M., & Bryant, P. J. (2005). A role for adenosine deaminase in
762 Drosophila larval development. *PLoS Biol, 3*(7), e201. doi:10.1371/journal.pbio.0030201
763 Dolezal, T., Gazi, M., Zurovec, M., & Bryant, P. J. (2003). Genetic analysis of the ADGF multigene
764 family by homologous recombination and gene conversion in Drosophila. *Genetics,*
765 *165*(2), 653-666.
766 Dolezelova, E., Nothacker, H. P., Civelli, O., Bryant, P. J., & Zurovec, M. (2007). A Drosophila
767 adenosine receptor activates cAMP and calcium signaling. *Insect Biochem Mol Biol,*
768 *37*(4), 318-329. doi:10.1016/j.ibmb.2006.12.003
769 Dolinar, K., Jan, V., Pavlin, M., Chibalin, A. V., & Pirkmajer, S. (2018). Nucleosides block AICAR-
770 stimulated activation of AMPK in skeletal muscle and cancer cells. *Am J Physiol Cell*
771 *Physiol, 315*(6), C803-C817. doi:10.1152/ajpcell.00311.2017

772 Domenici, M. R., Scattoni, M. L., Martire, A., Lastoria, G., Potenza, R. L., Borioni, A., . . . Popoli, P.
773 (2007). Behavioral and electrophysiological effects of the adenosine A2A receptor
774 antagonist SCH 58261 in R6/2 Huntington's disease mice. *Neurobiol Dis, 28*(2), 197-205.
775 doi:10.1016/j.nbd.2007.07.009
776 Dorn, R., & Krauss, V. (2003). The modifier of mdg4 locus in Drosophila: functional complexity is
777 resolved by trans splicing. *Genetica, 117*(2), 165-177. doi:Doi 10.1023/A:1022983810016
778 Dunwiddie, T. V., & Masino, S. A. (2001). The role and regulation of adenosine in the central
779 nervous system. *Annu Rev Neurosci, 24*, 31-55. doi:10.1146/annurev.neuro.24.1.31
780 Espinas, M. L., Jimenez-Garcia, E., Vaquero, A., Canudas, S., Bernues, J., & Azorin, F. (1999). The
781 N-terminal POZ domain of GAGA mediates the formation of oligomers that bind DNA
782 with high affinity and specificity. *J Biol Chem, 274*(23), 16461-16469.
783 doi:10.1074/jbc.274.23.16461
784 Fleischmannova, J., Kucerova, L., Sandova, K., Steinbauerova, V., Broz, V., Simek, P., & Zurovec,
785 M. (2012). Differential response of Drosophila cell lines to extracellular adenosine.
786 *Insect Biochem Mol Biol, 42*(5), 321-331. doi:10.1016/j.ibmb.2012.01.002
787 Fountain, S. J. (2013). Primitive ATP-activated P2X receptors: discovery, function and
788 pharmacology. *Front Cell Neurosci, 7*, 247. doi:10.3389/fncel.2013.00247
789 Fredholm, B. B. (2007). Adenosine, an endogenous distress signal, modulates tissue damage and
790 repair. *Cell Death Differ, 14*(7), 1315-1323. doi:10.1038/sj.cdd.4402132
791 Gianfriddo, M., Melani, A., Turchi, D., Giovannini, M. G., & Pedata, F. (2004). Adenosine and
792 glutamate extracellular concentrations and mitogen-activated protein kinases in the
793 striatum of Huntington transgenic mice. Selective antagonism of adenosine A2A
794 receptors reduces transmitter outflow. *Neurobiol Dis, 17*(1), 77-88.
795 doi:10.1016/j.nbd.2004.05.008
796 Giot, L., Bader, J. S., Brouwer, C., Chaudhuri, A., Kuang, B., Li, Y., . . . Rothberg, J. M. (2003). A
797 protein interaction map of Drosophila melanogaster. *Science, 302*(5651), 1727-1736.
798 doi:10.1126/science.1090289
799 Glass, M., Dragunow, M., & Faull, R. L. M. (2000). The pattern of neurodegeneration in
800 Huntington's disease: A comparative study of cannabinoid, dopamine, adenosine and
801 GABA(A) receptor alterations in the human basal ganglia in Huntington's disease.
802 *Neuroscience, 97*(3), 505-519. doi:Doi 10.1016/S0306-4522(00)00008-7
803 Gomes, C. V., Kaster, M. P., Tome, A. R., Agostinho, P. M., & Cunha, R. A. (2011). Adenosine
804 receptors and brain diseases: Neuroprotection and neurodegeneration. *Biochimica Et*
805 *Biophysica Acta-Biomembranes, 1808*(5), 1380-1399.
806 doi:10.1016/j.bbamem.2010.12.001
807 Guitart, X., Bonaventura, J., Rea, W., Orru, M., Cellai, L., Dettori, I., . . . Ferre, S. (2016).
808 Equilibrative nucleoside transporter ENT1 as a biomarker of Huntington disease.
809 *Neurobiol Dis, 96*, 47-53. doi:10.1016/j.nbd.2016.08.013
810 Han, S. K., Lee, D., Lee, H., Kim, D., Son, H. G., Yang, J. S., . . . Kim, S. (2016). OASIS 2: online
811 application for survival analysis 2 with features for the analysis of maximal lifespan and
812 healthspan in aging research. *Oncotarget, 7*(35), 56147-56152.
813 doi:10.18632/oncotarget.11269
814 Johnson, E. C., Kazgan, N., Bretz, C. A., Forsberg, L. J., Hector, C. E., Worthen, R. J., . . . Brenman,
815 J. E. (2010). Altered metabolism and persistent starvation behaviors caused by reduced
816 AMPK function in Drosophila. *PLoS One, 5*(9). doi:10.1371/journal.pone.0012799
817 Ju, T. C., Chen, H. M., Lin, J. T., Chang, C. P., Chang, W. C., Kang, J. J., . . . Chern, Y. (2011). Nuclear
818 translocation of AMPK-alpha1 potentiates striatal neurodegeneration in Huntington's
819 disease. *J Cell Biol, 194*(2), 209-227. doi:10.1083/jcb.201105010

Kao, Y. H., Lin, M. S., Chen, C. M., Wu, Y. R., Chen, H. M., Lai, H. L., . . . Lin, C. J. (2017a). Targeting ENT1 and adenosine tone for the treatment of Huntington's disease. *Hum Mol Genet, 26*(3), 467-478. doi:10.1093/hmg/ddw402

Kao, Y. H., Lin, M. S., Chen, C. M., Wu, Y. R., Chen, H. M., Lai, H. L., . . . Lin, C. J. (2017b). Targeting ENT1 and adenosine tone for the treatment of Huntington's disease. *Human Molecular Genetics, 26*(3), 467-478. doi:10.1093/hmg/ddw402

Knight, D., Harvey, P. J., Iliadi, K. G., Klose, M. K., Iliadi, N., Dolezelova, E., . . . Boulianne, G. L. (2010). Equilibrative nucleoside transporter 2 regulates associative learning and synaptic function in Drosophila. *J Neurosci, 30*(14), 5047-5057. doi:10.1523/JNEUROSCI.6241-09.2010

Krauss, V., & Dorn, R. (2004). Evolution of the trans-splicing Drosophila locus mod(mdg4) in several species of Diptera and Lepidoptera. *Gene, 331*, 165-176. doi:10.1016/j.gene.2004.02.019

Kucerova, L., Broz, V., Arefin, B., Maaroufi, H. O., Hurychova, J., Strnad, H., . . . Theopold, U. (2016). The Drosophila Chitinase-Like Protein IDGF3 Is Involved in Protection against Nematodes and in Wound Healing. *J Innate Immun, 8*(2), 199-210. doi:10.1159/000442351

Kucerova, L., Broz, V., Fleischmannova, J., Santruckova, E., Sidorov, R., Dolezal, V., & Zurovec, M. (2012). Characterization of the Drosophila adenosine receptor: the effect of adenosine analogs on cAMP signaling in Drosophila cells and their utility for in vivo experiments. *J Neurochem, 121*(3), 383-395. doi:10.1111/j.1471-4159.2012.07701.x

Kuo, Y., Ren, S., Lao, U., Edgar, B. A., & Wang, T. (2013). Suppression of polyglutamine protein toxicity by co-expression of a heat-shock protein 40 and a heat-shock protein 110. *Cell Death Dis, 4*, e833. doi:10.1038/cddis.2013.351

Lee, C. F., & Chern, Y. J. (2014). Adenosine Receptors and Huntington's Disease. *Adenosine Receptors in Neurology and Psychiatry, 119*, 195-232. doi:10.1016/B978-0-12-801022-8.00010-6

Lewis, E. A., & Smith, G. A. (2016). Using Drosophila models of Huntington's disease as a translatable tool. *J Neurosci Methods, 265*, 89-98. doi:10.1016/j.jneumeth.2015.07.026

Liu, H., Adebiyi, M., Liu, R. R., Song, A., Manalo, J., Wen, Y. E., . . . Xia, Y. (2018). Elevated ecto-5'-nucleotidase: a missing pathogenic factor and new therapeutic target for sickle cell disease. *Blood Adv, 2*(15), 1957-1968. doi:10.1182/bloodadvances.2018015784

Maier, S. A., Galellis, J. R., & McDermid, H. E. (2005). Phylogenetic analysis reveals a novel protein family closely related to adenosine deaminase. *J Mol Evol, 61*(6), 776-794. doi:10.1007/s00239-005-0046-y

Martinez-Mir, M. I., Probst, A., & Palacios, J. M. (1991). Adenosine-A2 Receptors - Selective Localization in the Human Basal Ganglia and Alterations with Disease. *Neuroscience, 42*(3), 697-706. doi:Doi 10.1016/0306-4522(91)90038-P

Medina-Pulido, L., Molina-Arcas, M., Justicia, C., Soriano, E., Burgaya, F., Planas, A. M., & Pastor-Anglada, M. (2013). Hypoxia and P1 receptor activation regulate the high-affinity concentrative adenosine transporter CNT2 in differentiated neuronal PC12 cells. *Biochem J, 454*(3), 437-445. doi:10.1042/BJ20130231

Melnikova, L., Kostyuchenko, M., Parshikov, A., Georgiev, P., & Golovnin, A. (2018). Role of Su(Hw) zinc finger 10 and interaction with CP190 and Mod(mdg4) proteins in recruiting the Su(Hw) complex to chromatin sites in Drosophila. *PLoS One, 13*(2), e0193497. doi:10.1371/journal.pone.0193497

866 Mievis, S., Blum, D., & Ledent, C. (2011). A2A receptor knockout worsens survival and motor
867 behaviour in a transgenic mouse model of Huntington's disease. *Neurobiol Dis, 41*(2),
868 570-576. doi:10.1016/j.nbd.2010.09.021
869 Mugat, B., Parmentier, M. L., Bonneaud, N., Chan, H. Y., & Maschat, F. (2008). Protective role of
870 Engrailed in a Drosophila model of Huntington's disease. *Hum Mol Genet, 17*(22), 3601-
871 3616. doi:10.1093/hmg/ddn255
872 Mutsuddi, M., Marshall, C. M., Benzow, K. A., Koob, M. D., & Rebay, I. (2004). The
873 spinocerebellar ataxia 8 noncoding RNA causes neurodegeneration and associates with
874 staufen in Drosophila. *Curr Biol, 14*(4), 302-308. doi:10.1016/j.cub.2004.01.034
875 Oughtred, R., Stark, C., Breitkreutz, B. J., Rust, J., Boucher, L., Chang, C., . . . Tyers, M. (2019). The
876 BioGRID interaction database: 2019 update. *Nucleic Acids Res, 47*(D1), D529-D541.
877 doi:10.1093/nar/gky1079
878 Picano, E., & Abbracchio, M. P. (2000). Adenosine, the imperfect endogenous anti-ischemic
879 cardio-neuroprotector. *Brain Res Bull, 52*(2), 75-82. doi:10.1016/s0361-9230(00)00249-5
880 Poernbacher, I., & Vincent, J. P. (2018). Epithelial cells release adenosine to promote local TNF
881 production in response to polarity disruption. *Nat Commun, 9*(1), 4675.
882 doi:10.1038/s41467-018-07114-z
883 Ruan, C. C., Kong, L. R., Chen, X. H., Ma, Y., Pan, X. X., Zhang, Z. B., & Gao, P. J. (2018). A(2A)
884 Receptor Activation Attenuates Hypertensive Cardiac Remodeling via Promoting Brown
885 Adipose Tissue-Derived FGF21. *Cell Metabolism, 28*(3), 476-+.
886 doi:10.1016/j.cmet.2018.06.013
887 Soltani-Bejnood, M., Thomas, S. E., Villeneuve, L., Schwartz, K., Hong, C. S., & McKee, B. D.
888 (2007). Role of the mod(mdg4) common region in homolog segregation in Drosophila
889 male meiosis. *Genetics, 176*(1), 161-180. doi:10.1534/genetics.106.063289
890 Song, W., Smith, M. R., Syed, A., Lukacsovich, T., Barbaro, B. A., Purcell, J., . . . Marsh, J. L. (2013).
891 Morphometric analysis of Huntington's disease neurodegeneration in Drosophila.
892 *Methods Mol Biol, 1017*, 41-57. doi:10.1007/978-1-62703-438-8_3
893 Soshnev, A. A., Baxley, R. M., Manak, J. R., Tan, K., & Geyer, P. K. (2013). The insulator protein
894 Suppressor of Hairy-wing is an essential transcriptional repressor in the Drosophila
895 ovary. *Development, 140*(17), 3613-3623. doi:10.1242/dev.094953
896 Steffan, J. S., Bodai, L., Pallos, J., Poelman, M., McCampbell, A., Apostol, B. L., . . . Thompson, L.
897 M. (2001). Histone deacetylase inhibitors arrest polyglutamine-dependent
898 neurodegeneration in Drosophila. *Nature, 413*(6857), 739-743. doi:Doi
899 10.1038/35099568
900 Stenesen, D., Suh, J. M., Seo, J., Yu, K., Lee, K. S., Kim, J. S., . . . Graff, J. M. (2013). Adenosine
901 nucleotide biosynthesis and AMPK regulate adult life span and mediate the longevity
902 benefit of caloric restriction in flies. *Cell Metab, 17*(1), 101-112.
903 doi:10.1016/j.cmet.2012.12.006
904 Swick, L. L., Kazgan, N., Onyenwoke, R. U., & Brenman, J. E. (2013). Isolation of AMP-activated
905 protein kinase (AMPK) alleles required for neuronal maintenance in Drosophila
906 melanogaster. *Biol Open, 2*(12), 1321-1323. doi:10.1242/bio.20136775
907 Thomas, S. E., Soltani-Bejnood, M., Roth, P., Dorn, R., Logsdon, J. M., Jr., & McKee, B. D. (2005).
908 Identification of two proteins required for conjunction and regular segregation of
909 achiasmate homologs in Drosophila male meiosis. *Cell, 123*(4), 555-568.
910 doi:10.1016/j.cell.2005.08.043
911 Toczek, M., Zielonka, D., Zukowska, P., Marcinkowski, J. T., Slominska, E., Isalan, M., . . .
912 Mielcarek, M. (2016). An impaired metabolism of nucleotides underpins a novel
913 mechanism of cardiac remodeling leading to Huntington's disease related

914 cardiomyopathy. *Biochim Biophys Acta, 1862*(11), 2147-2157.
915 doi:10.1016/j.bbadis.2016.08.019
916 Tyebji, S., Saavedra, A., Canas, P. M., Pliassova, A., Delgado-Garcia, J. M., Alberch, J., . . . Perez-
917 Navarro, E. (2015). Hyperactivation of D1 and A2A receptors contributes to cognitive
918 dysfunction in Huntington's disease. *Neurobiol Dis, 74*, 41-57.
919 doi:10.1016/j.nbd.2014.11.004
920 van Eyk, C. L., O'Keefe, L. V., Lawlor, K. T., Samaraweera, S. E., McLeod, C. J., Price, G. R., . . .
921 Richards, R. I. (2011). Perturbation of the Akt/Gsk3-beta signalling pathway is common
922 to Drosophila expressing expanded untranslated CAG, CUG and AUUCU repeat RNAs.
923 *Hum Mol Genet, 20*(14), 2783-2794. doi:10.1093/hmg/ddr177
924 Vazquez-Manrique, R. P., Farina, F., Cambon, K., Dolores Sequedo, M., Parker, A. J., Millan, J.
925 M., . . . Neri, C. (2016). AMPK activation protects from neuronal dysfunction and
926 vulnerability across nematode, cellular and mouse models of Huntington's disease. *Hum*
927 *Mol Genet, 25*(6), 1043-1058. doi:10.1093/hmg/ddv513
928 Vonsattel, J. P., & DiFiglia, M. (1998). Huntington disease. *J Neuropathol Exp Neurol, 57*(5), 369-
929 384. doi:10.1097/00005072-199805000-00001
930 Warrick, J. M., Chan, H. Y., Gray-Board, G. L., Chai, Y., Paulson, H. L., & Bonini, N. M. (1999).
931 Suppression of polyglutamine-mediated neurodegeneration in Drosophila by the
932 molecular chaperone HSP70. *Nat Genet, 23*(4), 425-428. doi:10.1038/70532
933 Xiao, C., Liu, N., Jacobson, K. A., Gavrilova, O., & Reitman, M. L. (2019). Physiology and effects of
934 nucleosides in mice lacking all four adenosine receptors. *PLoS Biol, 17*(3), e3000161.
935 doi:10.1371/journal.pbio.3000161
936 Yu, S., Waldholm, J., Bohm, S., & Visa, N. (2014). Brahma regulates a specific trans-splicing event
937 at the mod(mdg4) locus of Drosophila melanogaster. *RNA Biol, 11*(2), 134-145.
938 doi:10.4161/rna.27866
939 Zuberova, M., Fenckova, M., Simek, P., Janeckova, L., & Dolezal, T. (2010). Increased
940 extracellular adenosine in Drosophila that are deficient in adenosine deaminase
941 activates a release of energy stores leading to wasting and death. *Dis Model Mech, 3*(11-
942 12), 773-784. doi:10.1242/dmm.005389
943 Zurovec, M., Dolezal, T., Gazi, M., Pavlova, E., & Bryant, P. J. (2002). Adenosine deaminase-
944 related growth factors stimulate cell proliferation in Drosophila by depleting
945 extracellular adenosine. *Proc Natl Acad Sci U S A, 99*(7), 4403-4408.
946 doi:10.1073/pnas.062059699

947